



저작자표시-비영리-변경금지 2.0 대한민국

이용자는 아래의 조건을 따르는 경우에 한하여 자유롭게

- 이 저작물을 복제, 배포, 전송, 전시, 공연 및 방송할 수 있습니다.

다음과 같은 조건을 따라야 합니다:



저작자표시. 귀하는 원저작자를 표시하여야 합니다.



비영리. 귀하는 이 저작물을 영리 목적으로 이용할 수 없습니다.



변경금지. 귀하는 이 저작물을 개작, 변형 또는 가공할 수 없습니다.

- 귀하는, 이 저작물의 재이용이나 배포의 경우, 이 저작물에 적용된 이용허락조건을 명확하게 나타내어야 합니다.
- 저작권자로부터 별도의 허가를 받으면 이러한 조건들은 적용되지 않습니다.

저작권법에 따른 이용자의 권리는 위의 내용에 의하여 영향을 받지 않습니다.

이것은 [이용허락규약\(Legal Code\)](#)을 이해하기 쉽게 요약한 것입니다.

[Disclaimer](#)

**Master's Thesis**

**Distribution of dissolved organic  
radiocarbon in the Amundsen Sea,  
Antarctica**

남극 아문젠해 용존유기탄소의 방사성탄소 분포

**August 2016**

**Graduate School  
Seoul National University  
Earth and Environmental Sciences  
FANG, LING**

## ABSTRACT

Marine dissolved organic carbon (DOC), one of the largest reduced carbon pools, plays a crucial role in the global carbon cycle. Carbon isotopic abundances were used as a tracer to examine the source and fate of DOC in the Amundsen Sea, Antarctica.  $\Delta^{14}\text{C}$  values ranged between -260 ‰ and -481 ‰.  $\Delta^{14}\text{C}$  values were higher in the upper layer than in the deep layer and the highest  $\Delta^{14}\text{C}$  value was found in the Amundsen Sea polynya at a depth of 20m. The largest spatial variation of  $^{14}\text{C}$  age across the three stations was observed in the mixed layer.  $\Delta^{14}\text{C}$  values were significantly higher in the Amundsen polynya surface layer than in the sea ice zone while DOC concentration was only slightly higher, implying that a fraction of old DOC was removed in the upper layer. All samples collected from the Amundsen Sea were depleted in  $^{13}\text{C}$  throughout water column compared to the open oceans.  $\delta^{13}\text{C}$  values ranged from -26.2 to -28.9 ‰ with the mean value of  $-27.8 \pm 0.8$  ‰ (n=11). The  $\delta^{13}\text{C}$  and  $\Delta^{14}\text{C}$  distributions suggest that the Amundsen Sea polynya may be a sink of old DOC.

**Keywords:** dissolved organic carbon, radiocarbon, stable carbon isotope, polynya, Amundsen Sea

**Student Number:** 2014-25134

# TABLE OF CONTENTS

<b>ABSTRACT</b> .....	i
<b>TABLE OF CONTENTS</b> .....	ii
<b>LIST OF FIGURES</b> .....	iv
<b>LIST OF TABLES</b> .....	v
<b>1. INTRODUCTION</b> .....	<b>1</b>
1.1 Dissolved Organic Carbon.....	1
1.2 The Amundsen Sea .....	5
1.3 Objectives.....	8
<b>2. METHODS</b> .....	<b>10</b>
2.1 Sample Collection.....	10
2.1.1 Study Site.....	10
2.1.2 Sampling.....	13
2.2 Methodology.....	14
2.2.1 DOC Extraction Procedure.....	14
2.2.2 Performance Test of the Extraction System.....	17
2.3 DOC Isotope Analyses.....	23
2.3.1 Carbon Isotope Notation.....	23

2.3.2 Isotopic Ratio Analyses of Standards.....	24
<b>3. RESULTS .....</b>	<b>29</b>
3.1 $\Delta^{14}\text{C}$ Values of DOC.....	29
3.2 $\delta^{13}\text{C}$ Values of DOC.....	33
<b>4. DISCUSSION .....</b>	<b>35</b>
4.1 Distribution of Dissolved Organic Radiocarbon in the Amundsen Sea .....	35
4.2 The Sources of DOC in the Amundsen Sea.....	39
4.3 DOC Cycling of in the Deep Water Column.....	45
<b>5. SUMMARY AND CONCLUSION.....</b>	<b>49</b>
<b>6. REFERENCES .....</b>	<b>51</b>
<b>ABSTRACT (IN KOREAN) .....</b>	<b>64</b>

## LIST OF FIGURES

Figure. 1.	Map of the Amundsen Sea .....	12
Figure. 2.	The DOC extraction vacuum line sketch.....	16
Figure. 3.	Time series showing cumulative oxidized DOC concentration at each time point .....	20
Figure. 4.	Blank of UV extraction process at different irradiation time .....	21
Figure. 5	Recovery rate variation with DOC concentration.....	22
Figure. 6.	Profiles of $\Delta^{14}\text{C}$ values (A) and $\delta^{13}\text{C}$ values (B) at K1, K2 and K4 station .....	32
Figure. 7.	Distribution of $\delta^{13}\text{C}$ values in the Amundsen Sea .....	34
Figure. 8.	$\Delta^{14}\text{C}$ values of DOC plotted as a function of $\sigma_t$ .....	38
Figure. 9.	DOC cycling in the Amundsen Sea.....	343
Figure. 10.	Relationships between $\Delta^{14}\text{C}$ plot with $\delta^{13}\text{C}$ of DOC.....	44
Figure. 11.	Conceptual DOC cycling model.....	48

## LIST OF TABLES

Table 1.	Recovery rate.....	26
Table 2.	Radiocarbon standards.....	27
Table 3.	Stable carbon isotope standards.....	28
Table 4.	Isotope values of DOC.....	31

# 1. INTRODUCTION

## 1.1 Dissolved Organic Carbon

The operational definition of dissolved organic carbon (DOC) is being sufficiently small to pass through a filter with a nominal pore diameter of 0.2  $\mu\text{m}$  (and in some case, 0.7  $\mu\text{m}$ ) (McNichol and Aluwihare, 2007). DOC in the filtrate is a mixture between truly dissolved organic matter and colloidal fraction. Marine DOC represents one of the largest reduced carbon reservoirs on earth (~662 Gt C) and is comparable to the size of the atmospheric carbon pool (Hedges 1992; Hansell et al., 2009; Hansell et al., 2013). Previous studies have shown that DOC export through overturn of the water column can be an important contributor to the biological pump, approximately accounting for 20% of total organic carbon flux to the deep ocean (Ducklow et al., 2001; Hansell et al., 2009). Therefore, understanding the behavior of DOC is crucial to address the global carbon cycle. However, the biogeochemical cycle of DOC is still poorly understood after decades of research because of the limitation in its isolation and extraction.

Measured DOC concentrations in the surface water of the open ocean range from 50 to 80  $\mu\text{M}$  with higher DOC values observed at tropical and subtropical regions (Hansell et al., 2009). DOC concentrations are

nearly uniform at depths > 1000m (Williams and Druffel, 1987; Druffel et al., 1992; Bauer et al., 1998). Spatial gradients in the concentration of deep DOC was reported by Hansell and Carlson (1998): DOC concentration decreases from the North Atlantic (48  $\mu\text{M}$ ) to North Pacific (34  $\mu\text{M}$ ). Yet the mechanisms responsible for this decrease are not well understood.

It is commonly believed that most DOC in seawater originates from photosynthesis in the euphotic zone. Lines of evidence, like specific compound radiocarbon analyses and Keeling-plot using  $\Delta^{14}\text{C}$  values of DOC, have shown that the ultimate source of DOC is the in-situ primary production (Aluwihare et al., 2002; Mortazavi and Chanton, 2004; Repeta and Aluwihare, 2006). Annual global discharge of riverine DOC is around 0.25 Pg C (Hedges et al., 1997). Although riverine DOC accounts for only a small fraction of marine DOC, it is large enough to maintain steady state of the marine DOC reservoir based on the radiocarbon content (Williams and Druffel et al., 1987; Druffel et al., 1992). However, earlier studies of stable carbon isotope and lignin showed that most seawater DOC is more likely marine derived in the open ocean (Williams and Druffel, 1987; Opsahl and Benner, 1997). There are variety of processes through which a part of primary production is converted to DOC: extracellular release by phytoplankton (Carlson, 2002), bacterial production (McCarthy et al., 1998;

Ogawa et al., 2001), digestion and ingestion of zooplankton (Jumars et al., 1989), solubilization of particulate matter (Repeta and Aluwihare, 2006), and cell lysis by viruses (Carlson, 2002).

The ultimate sinks of DOC are poorly identified, and include bacterial degradation (Druffel et al., 1992; Hansell and Carlson 1998), photochemical degradation (Mopper et al., 1991), and adsorption to particles (Druffel and Williams, 1990; Hwang et al., 2006). The photochemical degradation has been proposed as the main process to remove refractory DOC, but the estimated loss rate cannot keep carbon mass balance with the estimated production rate (Mopper et al., 1991; Carlson, 2002). There was a hypothesis that the DOC gradient along the deep ocean conveyor was caused by slow bacterial remineralization (Hansell and Carlson, 1998). However, Hansell and Carlson (2013) recently suggested that deep DOC was generally conserved during the thermohaline circulation but with localized DOC sinks, such as in the North Pacific and subtropical Southern Ocean. Recently, an alternative mechanism proposed by Arrieta et al. (2015) demonstrated that the deep DOC avoids degradation because of its concentration falling below the threshold of microbes' utilization.

Radiocarbon ( $^{14}\text{C}$ ) and stable carbon ( $^{13}\text{C}$ ) natural abundances as tracers of time and origins have been used in studies of carbon cycling to

determine the sources and sinks of DOC, and provide information on the residence times and interaction among different carbon pools. The  $\Delta^{14}\text{C}$  values of DOC observed at surface in the open ocean ranged from -150 ‰ to -366 ‰ (Williams and Druffel, 1987; Bauer et al., 1992; Druffel et al., 1992; Druffel and Bauer, 2000; Druffel and Griffin, 2015).  $\Delta^{14}\text{C}$  values of DOC from the deep ocean ranged from -391 ‰ in the north Atlantic to -546 ‰ in the north Pacific. Meanwhile the apparent  $^{14}\text{C}$  ages of deep DOC increases from 4000 years to 6000 years along the deep-water mass circulation, indicating that deep DOC is removed at an extremely low rate (Williams and Druffel 1987; Bauer et al. 1992). The strong depletion in radiocarbon of deep DOC suggests that DOM in the deep ocean should be resistant to degradation and persist over multiple ocean mixing cycles. One outcome of previous work by using mass balance analysis based on the two-component conservative mixing model is that relatively low  $\Delta^{14}\text{C}$  values of surface DOC compared to suspended and sinking POC were caused by the mixing of surface-derived young DOC with old deep DOC reservoir (Druffel et al., 1992).

## 1.2 The Amundsen Sea

The Southern Ocean as a significant sink of atmospheric CO<sub>2</sub> plays an important role in global carbon cycle accounting for about 25% of the oceanic uptake of CO<sub>2</sub> (Takahashi et al., 2002). Especially the Antarctic continental shelf and coastal polynyas are highly productive (Roy et al., 2003; Sabine et al., 2004; Arrigo et al., 2008a). The primary production in the Antarctic was thought to be limited by Fe and light (Boyd, 2002). However, intense phytoplankton blooms have been occasionally observed in the austral summer. West Antarctica is going through rapid sea ice melting compared to east Antarctica (Stammerjohn et al., 2012). Additional iron released from sea ice and retreating glacier could stimulate photosynthesis in the euphotic zone, affecting the carbon cycling in this region (Coale et al., 2005; Poulton and Raiswell, 2005; Gerringa et al., 2012).

DOC concentrations in the upper mixed layer varied widely in the Antarctic: from 52 to 102 μM in the Brasfield and Gerlache Straits (Doval et al., 2002), 40 to 105 μM in the Weddell Sea (Wedborg et al., 1998), 41 to 72 μM in the Ross Sea (Carlson et al., 1998), and 52 to 63 μM in the Indian sector of the Southern Ocean (Wiebinga and de Baar, 1998). Compared to open sea water, much higher DOC concentrations (109 to >1158 μM) have been observed from sea ice and brine in the Arctic and Antarctic (Thomas et

al., 1995; Giannelli et al., 2001; Thomas et al., 2001). Given that the decrease of global sea ice inventory has been accelerating in recent years, some amount of DOC is expected to be released from melting sea ice and glaciers. Unfortunately, how this potentially enhanced phytoplankton bloom by sea ice melting and the basal grounding ice line retreat will affect the carbon cycle in the west Antarctic is not well studied due to the lack of in situ data.

The Amundsen Sea is located in the west Antarctic, characterized by a relatively shallow continental shelf, a large amount of perennial sea ice, and two highly productive coastal polynyas (Arrigo et al., 2003). This region is experiencing accelerated decrease in sea ice concentration and rapid retreating of the grounding ice line. Especially, Pine Island and the Thwaites Glacier are experiencing the highest loss rate (Rignot et al., 2008; Parkinson et al., 2012; Stammerjohn et al., 2012; Rignot et al., et al., 2014). The major reason for the recent sea ice melting is believed to be the intrusion of relatively warm modified Circumpolar Deep Water (mCDW) instead of the increase of atmospheric temperature (Jenkins et al., 2010; Jacobs et al., 2011). The Circumpolar Deep Water (CDW), which is relatively salty, warm and nutrient rich, intrudes into the eastern Amundsen Sea then flows southward to the Amundsen shelf driving sea ice melting

(Walker et al., 2007; Wåhlin et al., 2010; Jenkins et al., 2010). Understanding of the potential influence of sea ice melting in the Amundsen Sea is crucial to understand the biogeochemical carbon cycle in the Antarctic region. However, limitation of the observational data and the logistical difficulty to access the sea ice covered region hinders our understanding of this region (Yager et al., 2012).

Polynyas, seasonally open areas, gained a lot of attention due to the high primary productivity (Arrigo and van Dijken, 2003; Arrigo et al., 2008b; Arrigo et al., 2012). The Amundsen Sea harbors two highly productive polynyas, the Amundsen Sea Polynya (ASP), ~27,000 km<sup>2</sup>, and the Pine Island Polynya, ~18,000 km<sup>2</sup>. Especially, the ASP is the most productive polynya in the Antarctic in summer (Arrigo et al., 2012). Satellite data of mean chlorophyll-a concentration show that primary production in the ASP is 40% higher than the Ross Sea Polynya (Arrigo and van Dijken, 2003). Average annual NPP of the ASP is  $78.8 \pm 12.3 \text{ gCm}^{-2}\text{yr}^{-1}$  in the ASP (Arrigo et al., 2012). Particulate organic carbon flux mainly occurs in austral summer (Ducklow et al., 2015; Kim et al., 2015). Climate change is expected to affect the primary production in polynyas by increasing solar irradiation and nutrient supply. Much of our current understanding on the phytoplankton bloom in polynyas comes from studies

of remote sensing and sinking particle fluxes. DOM cycling, although crucial to complete the carbon cycling, is not well studied. DOC distribution has not been reported in the Amundsen Sea region, not to mention its isotopic ratios.

### **1.3 Objectives**

The Amundsen Sea is one of the regions seriously impacted by global warming and climate change. The biogeochemical cycle in the ASP may be significantly altered as the accelerated sea ice melting and stronger winds increase solar irradiation and nutrient supply. One of the main objectives of this study was to examine the DOC cycling on the Amundsen Shelf based on its carbon isotopes.

I measured carbon isotope contents of DOC samples collected from the Amundsen Sea during the summer 2013/2014 cruise. DOC was extracted via the UV-oxidation method (Beaupré et al., 2007). The stable carbon and radiocarbon isotope ratios of the UV-oxidized CO<sub>2</sub> were measured at National Ocean Sciences Accelerator Mass Spectrometry (AMS) Facility at Woods Hole Oceanographic institution (McNichol et al., 1994). Main questions addressed are:

- The spatial and vertical distribution of dissolved organic

radiocarbon in the sea ice zone and the highly productive Amundsen Sea polynya.

- The causes of spatial variability in DOC radiocarbon contents.
- Estimation of the amount that becomes accumulated in surface DOC in polynya during phytoplankton bloom.
- Identification of the sources and sinks of DOC in the water column.
- Ultimately, addressing the fate of DOC in the Antarctic margin.

## **2. METHODS**

### **2.1 Sample Collection**

#### **2.1.1 Study site**

The Amundsen Sea, Antarctica, has been occupied multiple times since 2009 by KOPRI (Korea Polar Research Institute). Various objectives, such as understanding the hydrographic characteristics, air-sea exchange, sea ice and glacier extent, and water circulation, were pursued in this project. Data presented here are from analyses of samples collected during the ANA04B cruise in December 2013-January 2014 in the Amundsen Sea.

The global warming will enhance the ocean stratification and accelerate melting of sea ice and glaciers, increasing the availability of light for photosynthesis (Boyd and Doney, 2002). In addition to the sunlight, climate condition, such as sea ice concentration and winds, strongly regulates the phytoplankton bloom in polynyas. Strong upwelling and wind-driven vertical turbulent mixing contribute significantly to nutrient supply to the euphotic zone. Considering that the sea ice melting rate is increasing (Rignot et al., 2002; Rignot et al., 2014), the influence of polynyas on organic carbon cycle is likely more significant in the future. Therefore, it is

important to constraint the carbon cycling inside the polynya and document how these changes may impact the Antarctic environment. Characteristics of POC export has been recently addressed (Ducklow et al., 2015; Kim et al., 2015). However, no DOC concentration and its carbon isotopic values haven been studied in the Amundsen Sea. Identifying the fate of DOC in the Antarctic under the changing climate will be beneficial to characterize the global carbon cycle. However, because of harsh environmental conditions and the lack of in-situ measurements, the status quo of DOC cycling and how it responses to the changing climate have not been studied in the Amundsen Sea (Yager et al., 2012).

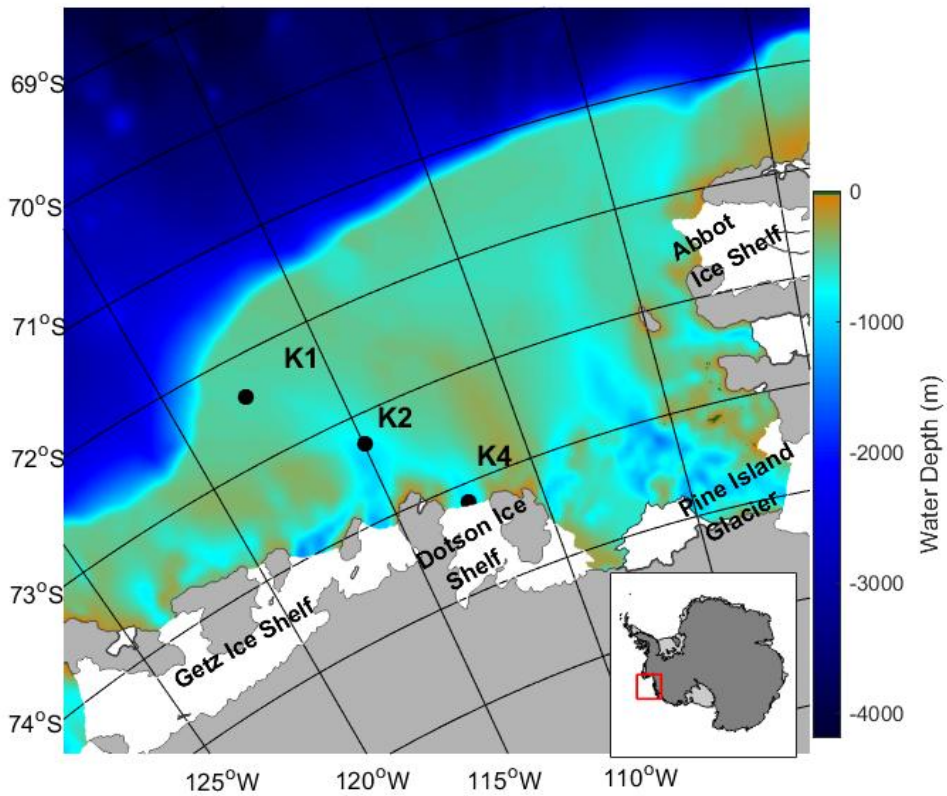


**Fig. 1.** Bathymetry map of the Amundsen Sea. K1, K2, and K4 are the sampling stations; K1 is located in the sea ice zone covered with year-round sea ice; K2 is located inside the Amundsen Sea Polynya; K4 is inside the polynya and near the Dotson Ice shelf.

### **2.1.2 Study site**

The stations are located in various surface water conditions from sea ice zone to the center of the ASP and near the Dotson Ice Shelf (Fig. 1), between 110°W and 120°W longitudinally and between 72°S and 74°S meridionally. Hydrographic information (salinity and temperature) was collected using a conductivity-temperature-depth (CTD) system mounted on a rosette.

Water samples both for DOC concentration and  $\Delta^{14}\text{C}$  measurement were collected at multiple depths using the rosette system equipped with 24 20L Niskin bottles. Seawater was gravity-filtered through 0.7  $\mu\text{m}$  Whatman quartz filter that were baked at 450°C for at least 4 h. The 500ml amber glass bottles were pre-cleaned with 10% HCl and rinsed with deionized water followed by baking at 450°C for at least 4 h. Sample bottles were flushed three times with filtered seawater before filling. The bottles were capped and stored frozen at -20 °C in dark before analysis. Samples were analyzed in October 2015. The depths of all samples collected from each station are listed in Table 4. Some samples were lost during transport and storage.

## **2.2. Methodology**

### **2.2.1 DOC extraction procedure**

Irradiation of samples by high energy ultraviolet was necessary to convert DOC to CO<sub>2</sub> for measurement of <sup>14</sup>C (Beaupré et al., 2007). Frozen samples were thawed by submerging the bottles in warm tap water and then poured into the quartz reactor, which was designed to interface directly to a vacuum line (Fig. 2). The vacuum manifold is connected to a rotary vane pump (Edwards Vacuum EM 18) through a molecular sieve trap (MDC Vacuum Products, Part No. 431003). After measurement of the volume of the sample in the reactor, the sample was acidified to pH 2-3 by adding 85% H<sub>3</sub>PO<sub>4</sub> with a pre-baked Pasteur pipette. The reactor was sealed with the 65/40 socket joint with 85% H<sub>3</sub>PO<sub>4</sub>. The reactor was placed on the magnetic stirrer inside the UV chamber and connected to the chiller, nitrogen gas supplying copper tubing and vacuum line. Then the sample was sparged with high purity nitrogen gas (99.999%) with a flow rate of 200ml/min until the concentration of CO<sub>2</sub> measured by the infrared CO<sub>2</sub> analyzer decrease to almost 0 for roughly 60 minutes. The DOC was oxidized to CO<sub>2</sub> with 1200 W UV for 6h. The irradiated sample then was sparged with N<sub>2</sub> again, which carries the CO<sub>2</sub> gas through a KIO<sub>3</sub> trap to remove Cl<sub>2</sub> gas, cryogenically purified at U-trap#1 (isopropyl alcohol-dry ice slush) and collected in U-trap

#2 (a 34.3 cm<sup>3</sup> calibrated volume) (Fig. 2). The amount of collected CO<sub>2</sub> was quantified by an absolute pressure gauge (MKS Corp.). Collected CO<sub>2</sub> was stored into 6-mm Pyrex tubes.

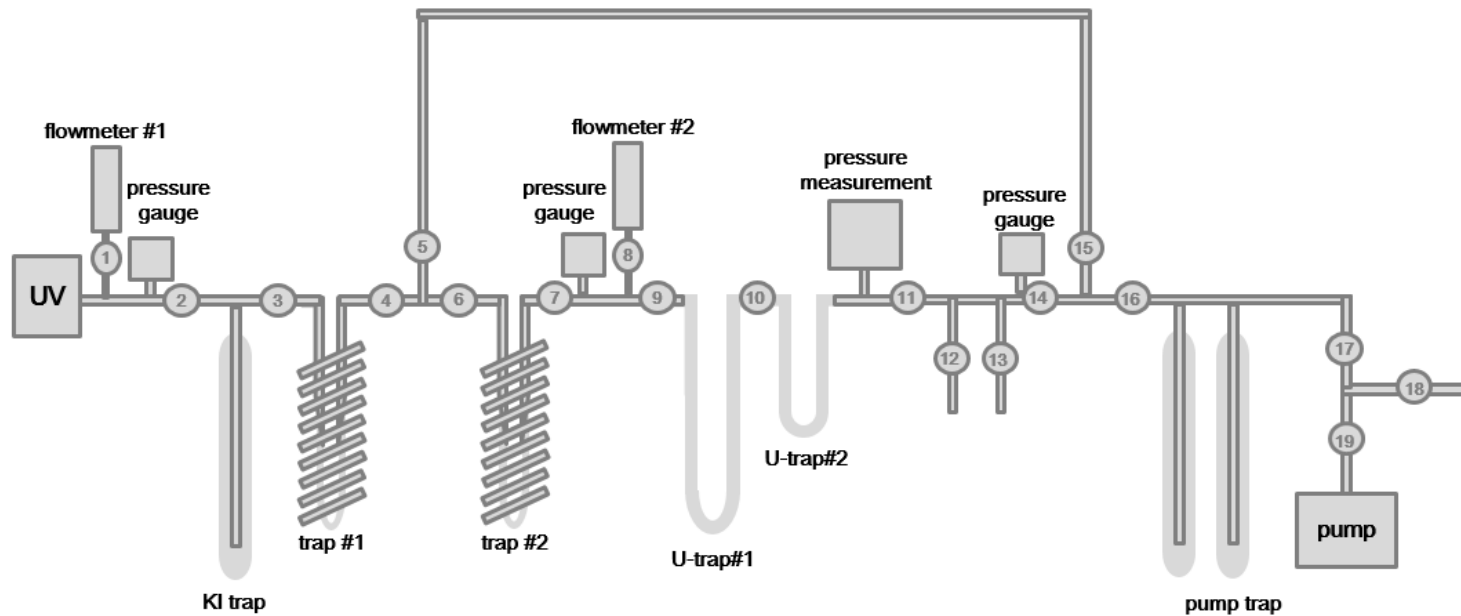


**Fig. 2.** The DOC extraction vacuum line sketch. The circles with numbers inside indicate stopcocks.

## **2.2.2 Performance test of the extraction system**

### **2.2.2.1 Time series irradiation**

Time series irradiation test was performed to decide optimal irradiation time to recover most of DOC that can be representative of the bulk radiocarbon age. Surface waters from the west coast of Korea and deep water from the East Sea were used as a working standard. The produced CO<sub>2</sub> after certain time intervals were quantified for DOC (Fig. 3). Most of DOC was oxidized within the first 2 hours and the CO<sub>2</sub> collected in the fifth and sixth hour of irradiation accounted for only 1.6% and 0.5% of total cumulative yields, respectively (Fig. 3). As mentioned in Beaupre et al (2007), recovery rate for this experiments are 89% and 95%, all smaller than 100%, likely due to incomplete oxidation. DOC concentration and  $\Delta^{14}\text{C}$  were reported to be insensitive to irradiation time after 2 hours (Beaupre et al., 2007). However, in order to prevent excessive inclusion of blank 6 hours was chosen for UV irradiation in the experiments.

### **2.2.2.2 Blank**

The average of total blank was determined to be  $\sim 8 \pm 8 \mu\text{g C}$  (n=11) by reprocessing previously irradiated water (both ultrapure water and seawater). The CO<sub>2</sub> introduced by N<sub>2</sub> gas decreased from 3  $\mu\text{g C}$  to 0.8  $\mu\text{g C}$  by

changing from 4-nine N<sub>2</sub> gas to higher-purity N<sub>2</sub> gas (99.999%). A significant improvement in reducing blank amount was obtained when the marias on the vacuum line and the reactor were modified (Fig. 4). Marias were designed to stop UV travel inside the wall of glass tubing to protect the o-ring inside the UltraTorr fitting from UV irradiation since degradation of o-rings can contribute to carbon blank. The modified bigger marias effectively decreased the carbon blank from an average of 67 µg C (n=12) to 8 µg C (n=11). Other sources of blank carbon are unclear.

### **2.2.2.3 Recovery rate**

The performance of the UV extraction system was tested by multiple working standards (Table 1). Two monosaccharides, glucose and galactose, showed an average yield about  $91 \pm 6\%$  (n=12). Average recovery of surface and deep sea water was  $92 \pm 4\%$  (n=3). Noticeably, the recovery of the Korean East Sea deep water (the concentration measured with a TOC instrument (Shimadzu TOC-VCPH) was 54 µM), ~95%, is significantly higher than surface water from the west coast (120 µM), ~85%. There was a negative correlation between glucose concentration and recovery (fig. 5 A). This correlation became weaker if all processed DOC working standards were considered (fig. 5 B), indicating that in addition to concentration there

may be some other factors affecting the UV irradiation efficiency, such as chemical composition. Carbon isotopic standards, OX-I and Glucose, were also processed to evaluate the UV extraction system

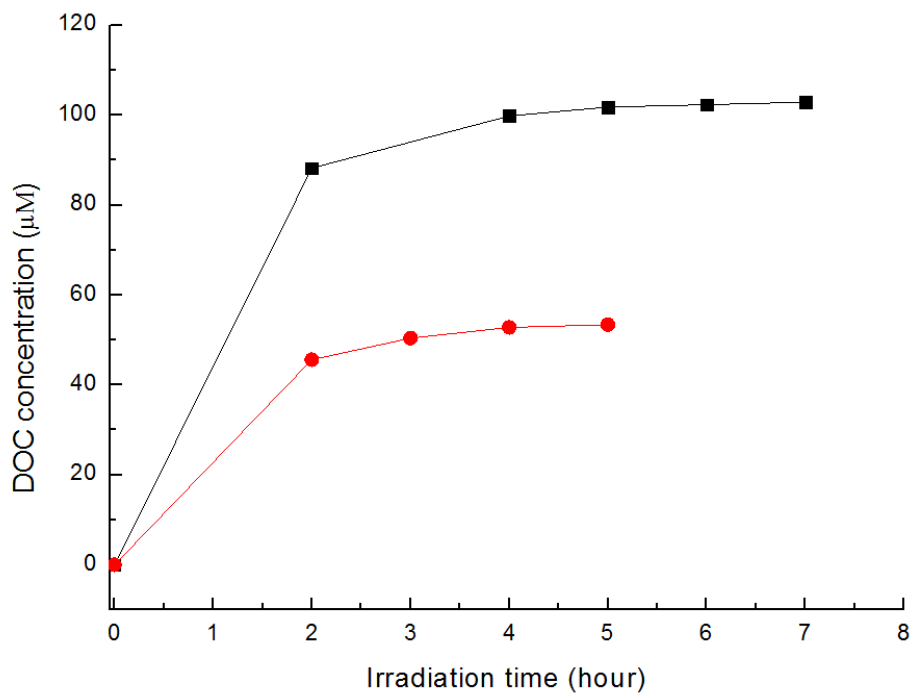


**Fig. 3.** Time series showing cumulative oxidized DOC concentration at each time point. Surface water collected from the west coast of Korea (squares) and deep water from the East Sea deep (circles) were used.

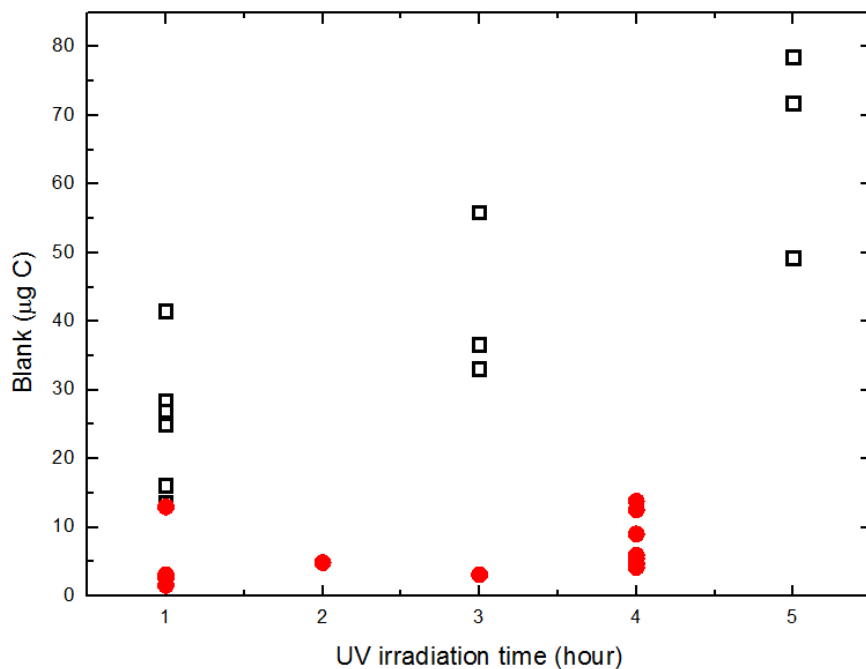


**Fig. 4.** Blank of UV extraction process at different irradiation time via unmodified line and reactor (open black squares) and modified line and reactor (filled red circles).

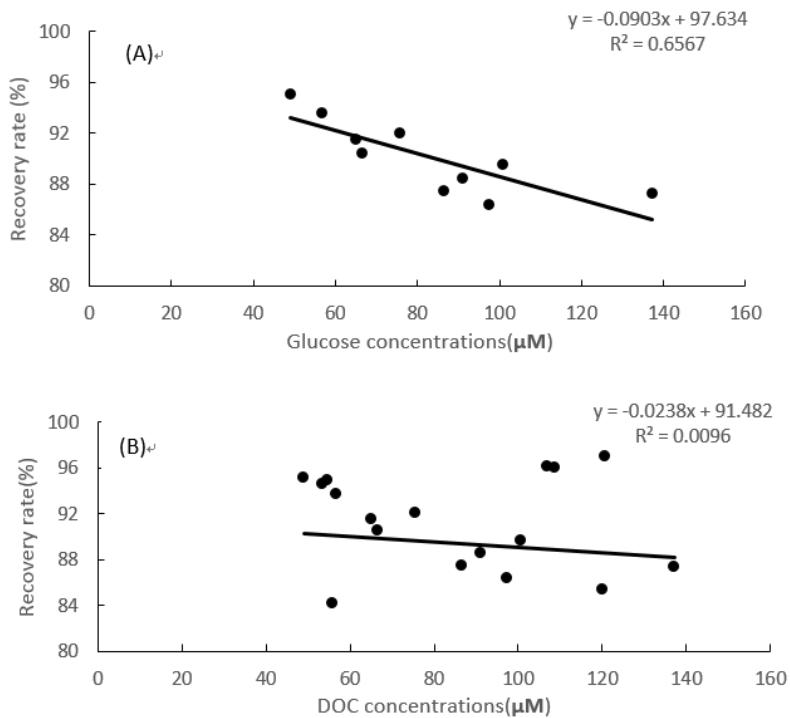
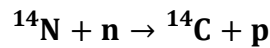


**Fig. 5.** Recovery variation with DOC concentration. (A) Recovery shows a strong negative correlation with concentration when only glucose was considered; (B) Recovery with respect to DOC concentrations of all processed working standards.

## 2.3. DOC isotope analyses

### 2.3.1. Carbon isotope notation

Along the 15 carbon isotopes (Lide, 2007),  $^{12}\text{C}$  and  $^{13}\text{C}$  are stable, and  $^{14}\text{C}$  are radioactive undergoes beta decay (Calvin et al., 1949) with a half-life of 5730 years (Godwin, 1962).  $^{14}\text{C}$  is naturally produced by the reaction of nitrogen with cosmic rays through the following reaction (Libby, 1955):



Nuclear weapons testing in the 1950s and 1960s dramatically increased the global  $^{14}\text{C}$  inventory (Suess, 1955).

Carbon isotope measurements are commonly reported compared to the ratio of  $^{14}\text{C}/^{12}\text{C}$  (or  $^{13}\text{C}/^{12}\text{C}$ ) in standard:

$$\delta^{13}\text{C} = \left[ \frac{^{13}\text{R}_{\text{sample}}}{^{13}\text{R}_{\text{standard}}} - 1 \right] \times 1000$$

Where  $^{13}\text{R}_{\text{sample}}$  and  $^{13}\text{R}_{\text{standard}}$  are  $^{13}\text{C}/^{12}\text{C}$  of sample and standard, respectively.

Radiocarbon content will reflect isotopic fractionation as well as radioactive decay. Therefore, a  $^{14}\text{C}$  isotopic ratio should be corrected for isotopic fractionation by normalization to a  $\delta^{13}\text{C}$  of -25‰:

$$\text{FM}_{\delta^{13}\text{C}} = \text{FM} \left[ \frac{(1 - 25/1000)}{(1 + \delta^{13}\text{C}/1000)} \right]^2$$

Where FM stands for fraction of modern carbon.  $FM_{\delta^{13}C}$  is fractionation-corrected FM.

The  $\Delta^{14}C$ , defined as the deviation in parts per thousand from the  $^{14}C$  activity of the nineteenth century wood, is corrected for fractionation using the  $\delta^{13}C$  of -25‰ (Stuiver and Polach, 1977):

$$\Delta^{14}C = [FM_{\delta^{13}C} \times e^{\lambda(1950-y)} - 1] \times 1000$$

Where  $\lambda = 1.201 \times 10^{-4}$  is the decay constant for radiocarbon and  $y$  is the sample collection year.

### **2.3.2. Isotopic ratio analyses of standards**

The radiocarbon and stable isotopic contents were measured at National Ocean Sciences Accelerator Mass Spectrometry (AMS) Facility at Woods Hole Oceanographic institution following standard protocol (McNichol et al., 1994). The  $CO_2$  for  $^{14}C$  measurement was converted to graphite in an  $H_2$  atmosphere over Co catalyst at NOSAMS.

OX-I and glycine were processed in the same way as samples as  $\Delta^{14}C$  modern and dead carbon standard, respectively.  $\Delta^{14}C$  values of OX-I were  $21 \pm 0.2$  ‰ (n=2) and  $\Delta^{14}C$  values of glycine were  $-970 \pm 0.5$  ‰ (n=2) (Table 2). These measurements were done at the W.M. Keck Carbon Cycle Accelerator Mass Spectrometer facility at UC Irvine. Uncertainties

(standard deviation of duplicate sample results) of  $\Delta^{14}\text{C}$  were 1.7 ‰ for OX-I, and 1.0 ‰ for glycine. The  $\Delta^{14}\text{C}$  measurements of OX-I and glycine concurrently deviated about 30 ‰ from expected values. However, the  $\Delta^{14}\text{C}$  values of duplicate samples had a precision within 1‰ suggesting that the impact of blank appears to remain constant. Using a mass balance approach, the blank amount is estimated to be 12.4  $\mu\text{gC}$  with a radiocarbon value of -369‰. Blank corrections for  $\Delta^{14}\text{C}$  values of samples were based on this.

D-glucose and glycine as  $\delta^{13}\text{C}$  working standards were processed on the DOC extraction system as well. The  $\delta^{13}\text{C}$  values of D-glucose and glycine determined by combustion were -9.8‰ and -40.4‰ respectively (Table 3). Expected  $\delta^{13}\text{C}$  values of these standards processed by the UV irradiation system were  $-11.3 \pm 0.4\text{‰}$  (n=2) and  $-39.6 \pm 0.3\text{‰}$  (n=2) for D-glucose and glycine, respectively. Our results indicated that the fractionation effect of UV oxidation is within 2‰ from the true value.

**Table 1.** Recovery

DOC Sample	Expected concentrations ( $\mu\text{M}$ )	Measured concentrations ( $\mu\text{M}$ )	Recovery (%)
Glucose	66.7	60.3	90.5
Glucose	65.1	59.5	91.5
Glucose	137.3	119.8	87.3
Glucose	69.2	63.3	91.6
Glucose	100.9	90.4	89.6
Glucose	91.2	80.7	88.5
Glucose	86.7	75.8	87.4
Glucose	75.8	69.7	92.0
Glucose	97.6	84.2	86.3
Glucose	49.1	46.7	95.1
Galactose	106.9	102.8	96.1
Glycine	120.7	117.0	96.9
Glycine	108.9	104.4	95.9
OX-1	56.0	47.2	84.1
OX-1	78.2	58.6	75.0
OX-1	91.0	68.6	75.1
Surface seawater	120.2	102.7	85.3
Deep seawater	54.7	51.9	94.9
Deep seawater	53.6	50.7	94.6

**Table 2.** Radiocarbon standards

Sample	Expected $\Delta^{14}\text{C}(\text{‰})$	Measured $\Delta^{14}\text{C}(\text{‰})$
OX-1	49	20.8, 21.2
Glycine	-1000	-970.0, -969.5

**Table 3.** Stable carbon isotope standards

Sample	Expected $\delta^{13}\text{C}$ (‰)	Measured $\delta^{13}\text{C}$ (‰)
D-glucose	-9.8	-11.0, -11.7
Glycine	-40.4	-39.9, -39.9

## 3. RESULTS

### 3.1 $\Delta^{14}\text{C}$ values of DOC

The  $\Delta^{14}\text{C}$  values of DOC from sea ice zone (Station K1), the Amundsen Sea polynya (Station K2), and the Dotson Ice Shelf site (Station K4) ranged from -260‰ in the upper layer of the ASP to -481‰ in the sea ice zone bottom water (Fig. 6A; Table 3). In the mixed layer,  $\Delta^{14}\text{C}$  values were significantly higher in the polynya followed by the Dotson ice shelf site and lowest in the sea ice zone. The youngest DOC (-260‰) was found at a depth of 20m in the polynya. Significant spatial variability in  $\Delta^{14}\text{C}$  results was observed in the surface water, ranging between -284‰ and -425‰.  $\Delta^{14}\text{C}$  values in the sea ice zone and the polynya converged to a similar value at the depth >400m. Compared with the surface water,  $\Delta^{14}\text{C}$  values in the deep water varied within a relatively small range, around 64‰.

The vertical profiles of  $\Delta^{14}\text{C}$  values were different among the three stations reflecting the difference in primary production, turbulent diffusion, and/or water mixing (Fig. 6A). Generally, for each station, the  $\Delta^{14}\text{C}$  values of DOC were highest in the shallow water and decreased with increasing depth. However,  $\Delta^{14}\text{C}$  values were more variable throughout the water

column in the polynya than in the sea ice zone. The  $\Delta^{14}\text{C}$  value in the polynya, Station K2, slightly increased from -284‰ at the surface to -260‰ at a depth of 20m, then  $\Delta^{14}\text{C}$  values decrease to -301‰ at 400m and decreased to the minimum (-477‰) at the bottom.

Except for the bottom water,  $\Delta^{14}\text{C}$  values in the sea ice zone (Station K1) were significant lower than in the polynya and neat the Dotson Ice Shelf. At the depth near the bottom, the  $\Delta^{14}\text{C}$  value of sea ice zone (-481‰) was close to the corresponding  $\Delta^{14}\text{C}$  in the polynya (-477‰), but the  $\Delta^{14}\text{C}$  value at deep depth near the Dotson Ice Shelf was higher by 64‰. The  $\Delta^{14}\text{C}$  value of bottom samples collected in the sea ice zone was similar to the published Southern Ocean  $\Delta^{14}\text{C}$  values at the depth 400-800m, where the Circumpolar Deep Water (CDW) is located (Druffel and Griffin, 2015). This similarity in  $\Delta^{14}\text{C}$  is consistent with intrusion of the CDW and/or mCDW onto the Amundsen Shelf.

The DOC concentration was estimated based on the mean sea water recovery and the recovered amount from DOC-oxidation. The estimated DOC concentrations ranged from 42 to 64 ( $\pm 10$ )  $\mu\text{M}$ . Although the estimated DOC concentration have a large uncertainty, these values are comparable to the results obtained independently (Jung et al., in preparation).

**Table 4.** Isotope values of DOC

Station	Depth(m)	$\Delta^{14}\text{C}$ (‰)	$\delta^{13}\text{C}$ (‰)	Estimated [DOC] ( $\mu\text{M}$ )
K1	25	-425	-27.0	53
	200	-470	-27.0	50
	500	-481	-28.5	44
K2	0	-284	-29.0	64
	20	-260	-28.7	62
	80	-301	-28.5	40
	400	-309	-28.1	43
	630	-444	-27.5	42
	830	-477	-26.6	45
K4	0	-337	-28.6	58
	40	-402	-26.2	44
	770	-417	-27.9	53

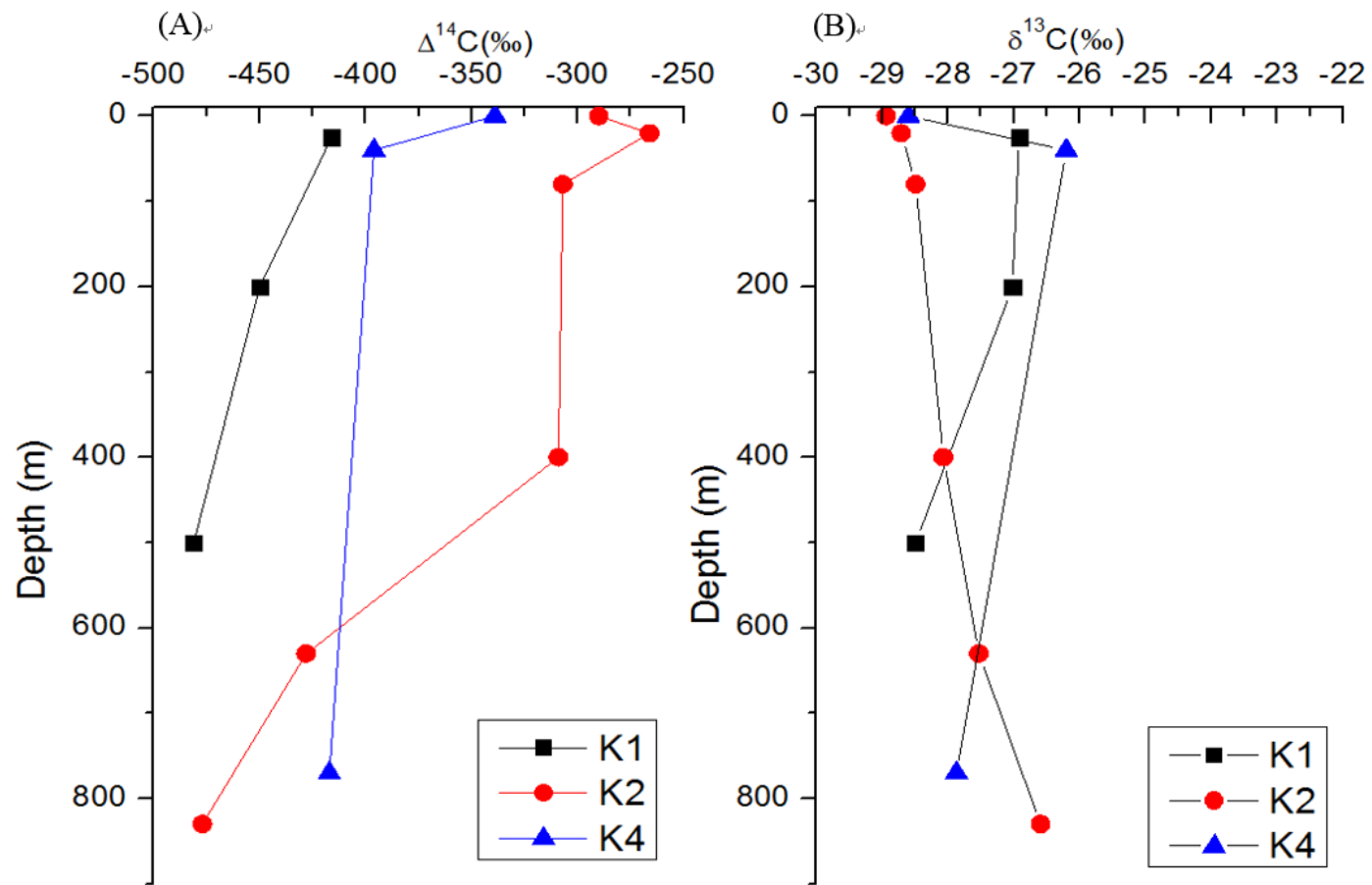


**Fig. 6.** Profiles of (A)  $\Delta^{14}\text{C}$  values and (B)  $\delta^{13}\text{C}$  values at K1, K2 and K4 stations.

### 3.2 $\delta^{13}\text{C}$ values of DOC

DOC  $\delta^{13}\text{C}$  values in the Amundsen Sea ranged from -26.2 to -28.9‰ with an average of  $-27.8 \pm 1.9\text{‰}$  (n=12) (Fig. 6). These values are considerably lower than the values observed in the open ocean (Druffel et al., 1992; Bauer et al., 1998; Druffel and Griffin, 2015). The  $\delta^{13}\text{C}$  values in the surface water were similar to that of suspended POC in the polynya and near Dotson Ice Shelf (Kim et al., 2015). Immediately below the surface,  $\delta^{13}\text{C}$  measurements diverged at three stations.

There is no apparent pattern in  $\delta^{13}\text{C}$  profiles across all three sites. The  $\delta^{13}\text{C}$  values increased monotonically with increasing depth in the polynya by  $\sim 2.3 \text{‰}$ . In the upper  $\sim 400\text{m}$  layer, the  $\delta^{13}\text{C}$  values in the polynya were lower than at the other stations.

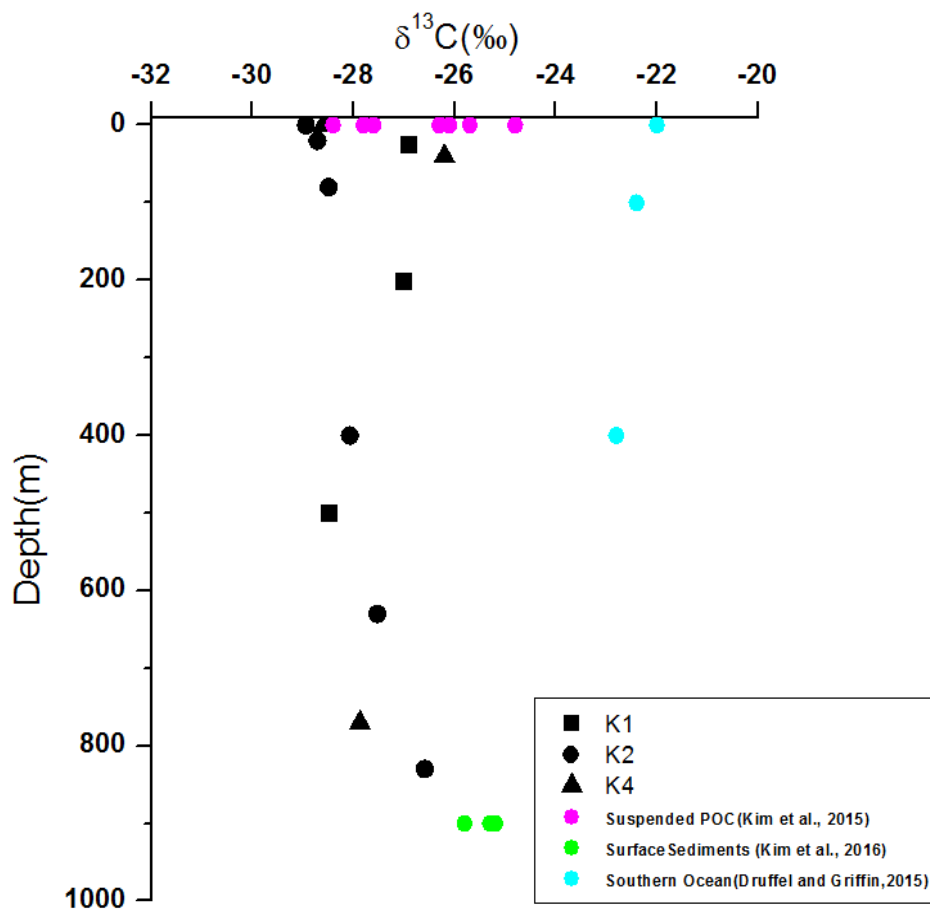


**Fig. 7.**  $\delta^{13}\text{C}$  values of DOC (this study), suspended POC (Kim et al., 2015), surface sediments (Kim et al., 2016) in the Amundsen Sea and those from Southern Ocean (Druffel and Griffin, 2015).

## 4. DISCUSSION

Studies showed that sea ice retreating has been accelerating in the West Antarctic (Rignot et al., 2008; Rignot et al., 2014). This rapid change in sea ice concentration and ice shelf retreat in the Amundsen Sea provides an opportunity to study how this change will impact the biogeochemical cycle of DOC in the Amundsen Sea. In this section, I try to determine the source and fate of DOC based on carbon isotopic signatures. This examination reveals some new insights to the fate of old refractory DOC in the water column.

### 4.1 Distribution of dissolved organic radiocarbon in the Amundsen Sea

Greatest spatial variability in  $\Delta^{14}\text{C}$ -DOC was found in the shallow water:  $\Delta^{14}\text{C}$  values increased from -425‰ in the sea ice zone to -284‰ in the polynya (fig. 6A). When  $\Delta^{14}\text{C}$  values are plotted as a function of density ( $\sigma_t$ ), observed spatial variation of  $\Delta^{14}\text{C}$  in the shallow water across the three stations can be partly explained by the isopycnal mixing process (Fig. 8). However, the scattered  $\Delta^{14}\text{C}$  values at the same density indicate that other processes must play a significant role in the distribution of dissolved organic

radiocarbon as well. Except for the Dotson Ice Shelf site,  $\Delta^{14}\text{C}$  of deep water is generally conserved with an average of  $-479\text{‰}$ . The anomaly in the deep water of the Dotson Ice Shelf suggests additional young DOC sources near the ice shelf and/or strong vertical mixing.

Phytoplankton bloom is intense in the Antarctic polynyas when sea ice opens during the austral summer. Especially, the highest productivity was observed in the ASP (Arrigo et al., 2012; Arrigo et al., 2008). However, the difference in DOC concentration in the surface waters between the Amundsen polynya and sea ice zone was only  $9\ \mu\text{M}$ . Instead the  $\Delta^{14}\text{C}$  values at the surface in the Amundsen polynya were higher than in the sea ice zone. At any given depth, the highest  $\Delta^{14}\text{C}$  value was observed in the polynya. Significant increase in  $\Delta^{14}\text{C}$  but small increase in DOC concentration in the surface layer of the polynya may not appear intuitive.

One explanation may be that the photosynthesis-derived supply of DOC is insignificant in the Amundsen Sea because only small proportion of total organic carbon is partitioned into DOC, which was observed in the Ross Sea (Carlson et al., 1998). However, the reported DOC concentration in the Amundsen polynya surface could rise to  $>100\ \mu\text{M}$  during the phytoplankton bloom (Sipler and Connelly, 2015). Another possibility is that DOC does not accumulate in the polynya euphotic layer at our sampling

time because of high DOC consumption rate. High primary production in the polynya increases the input of DOC to stimulate bacterial activity, which in turn, enhances the remineralization of DOC.

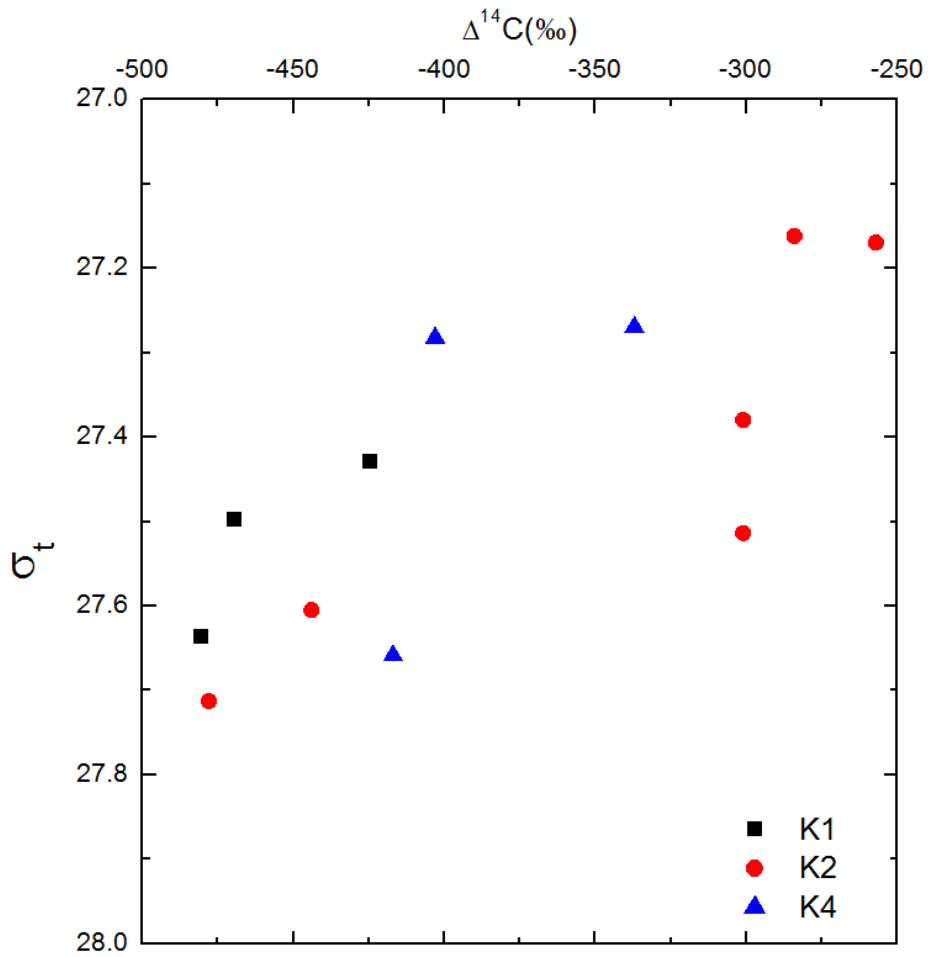


**Fig. 8.**  $\Delta^{14}\text{C}$  values of DOC plotted as a function of  $\sigma_t$ . There is a strong correlation between density and  $\Delta^{14}\text{C}$  values, but the variation in  $\Delta^{14}\text{C}$  values at same density cannot be explained by mixing process.

## 4.2 The sources of DOC in the Amundsen Sea

The DOC introduced by CDW to the deep layer of the sea ice zone mixes with DOC released from sediment and sinking particle (Fig. 9), while the deep DOC is continually transported southward along the current. Near the ice shelf, DOC is modified by the input of glacial meltwater and rises to the surface layer. Based on the DOC concentration and  $\Delta^{14}\text{C}$  values, the input from the seafloor seems negligible but meltwater would slightly alter the DOC characteristics near the ice shelf. In order to approximately estimate the sources to the DOC in the surface water, I assume that the surface water DOC was mainly comprised of labile and semilabile DOC from recent primary production and refractory old DOC supplied via upwelling. My approach is to back-calculate the  $\Delta^{14}\text{C}$ -DOC added to achieve the  $\Delta^{14}\text{C}$  value in the surface water of the Amundsen polynya. For example, if the background (aged and refractory) DOC has a concentration of 44  $\mu\text{M}$  in the sea ice zone with a  $\Delta^{14}\text{C}$  value of -481‰ throughout the water column, and average surface DOC concentration is 53  $\mu\text{M}$  with  $\Delta^{14}\text{C}$  value of -425‰, then the required DOC input will be 9  $\mu\text{M}$  ( $53-44 = 9 \mu\text{M}$ ) with a  $\Delta^{14}\text{C}$  value of -151‰ [ $9 \times (-151‰) + 44 \times (-481‰) = 53 \times (-425‰)$ ]. This estimated  $\Delta^{14}\text{C}$  value is close to the  $\Delta^{14}\text{C}$  value of dissolved inorganic carbon, around -150‰, implying that photosynthesis-derived DOC input is the main source

of surface DOC in the sea ice zone.

When the same calculation was repeated for the Amundsen Sea polynya and Dotson Ice Shelf station, the additional inputs needed to satisfy the mass balances are 18  $\mu\text{M}$  with a  $\Delta^{14}\text{C}$  value of 230 ‰ and 5  $\mu\text{M}$  with a  $\Delta^{14}\text{C}$  value of 426 ‰, respectively. Apparently, the calculated radiocarbon values are unrealistically high suggesting that two-component model does not work at these stations. The differences between the sea ice zone and the polynya may imply that DOC cycling in the Amundsen Sea is much more complicated compared to the open ocean.

Identifying the sources of deep DOC in the Amundsen Sea is challenging due to lack of concentration and isotopic data. Circumpolar deep water (CDW) and modified CDW (mCDW) as the main contributors of deep DOC are expected to transport highly decomposed, low concentration, old DOC to the Amundsen Sea bottom water. Sampling of CDW and mCDW will be crucial to understand the radiocarbon and stable isotope distribution of DOC in the Amundsen Sea. Without the DOC observation data at CDW, I compared my results with a Southern Ocean site, which is nearest to my station. The  $\Delta^{14}\text{C}$  value obtained from the Southern Ocean is about -500‰ to -480‰ at the depth of CDW (Druffel and Griffin, 2015).  $\Delta^{14}\text{C}$  values of the bottom water in the sea ice zone and the

Amundsen polynya were  $-481\text{ ‰}$  and  $-477\text{ ‰}$ , which are similar to or slightly higher than the values of the Southern Ocean. This similarity in  $\Delta^{14}\text{C}$  is consistent with the current understanding on the CDW intrusion onto the shelf. However,  $\Delta^{14}\text{C}$  value of deep DOC at the Dotson Ice Shelf station ( $\sim -417\text{ ‰}$ ) was much higher than at the other two stations. This increase in  $\Delta^{14}\text{C}$  implies addition of young DOC near the ice shelf station. The potential young DOC sources in the deep water near the ice shelf may include conversion of sinking POC and release from the sediment. Besides, measured young radiocarbon age in the deep water maybe a result of strong vertical mixing.

There may exist two distinctive types of sources to DOC in the Amundsen Sea based on the  $\Delta^{14}\text{C}-\delta^{13}\text{C}$  plot (Fig. 10). One is young in radiocarbon ages with a narrow  $\delta^{13}\text{C}$  variation. The average of  $\delta^{13}\text{C}$  value ( $28.5\pm 0.3\text{ ‰}$ ) is similar to suspended POC, implying that photosynthesis-derived DOC input is a dominant young DOC source. Another type is depleted in radiocarbon with a larger variability in  $\delta^{13}\text{C}$  values. There may be multiple old sources with various stable carbon isotope contributing to the deep DOC. Potential sources of deep DOC include refractory DOC introduced by mCDW and CDW, released from sediment and sinking POC. To quantify the proportion of each source, additional data of sediment pore

water and seawater at the Amundsen Sea, mCDW and CDW regions are needed.

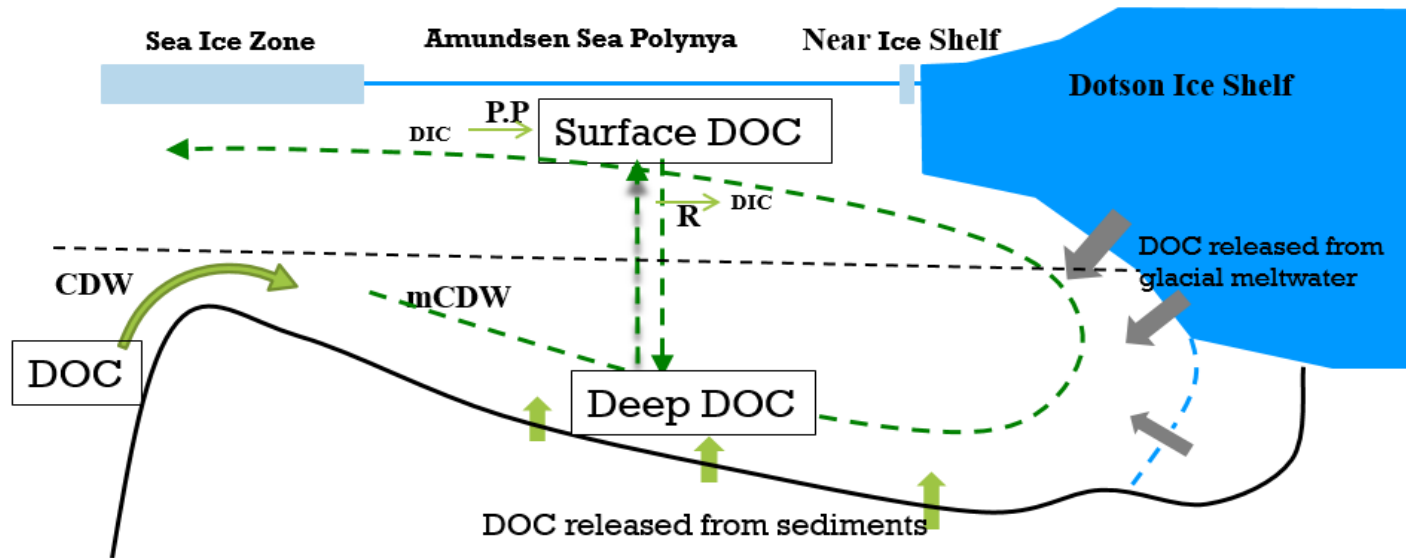


**Fig. 9.** DOC cycling in the Amundsen Sea

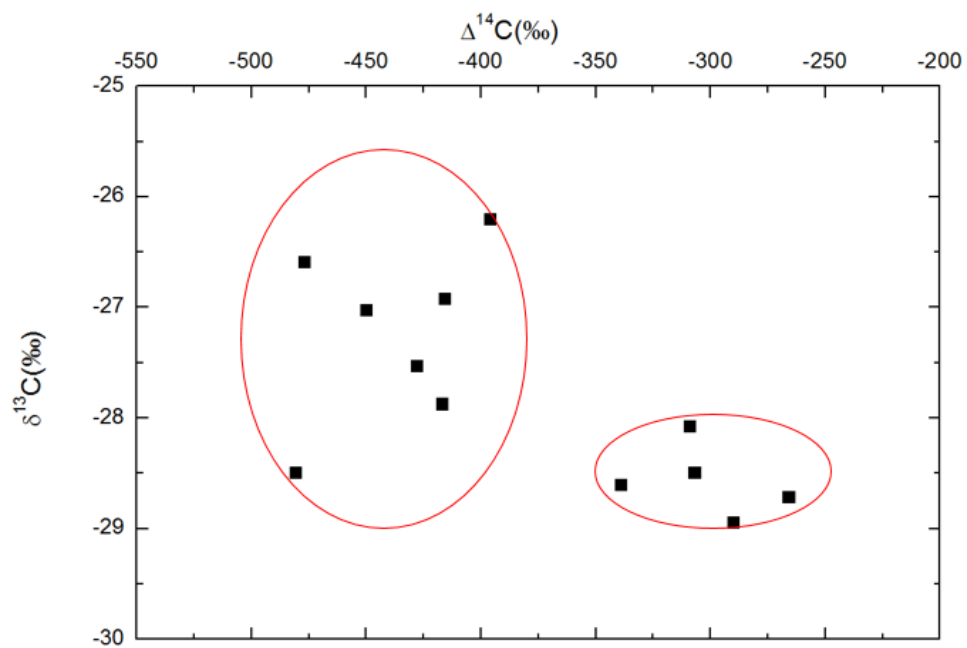


**Fig. 10.** Relationships between  $\Delta^{14}\text{C}$  plot with  $\delta^{13}\text{C}$  of DOC.

### 4.3 Old DOC cycling in the water column

Inside the Amundsen Sea polynya, primary production is likely the dominant young DOC input in the euphotic zone. The average concentration of deep DOC as background of refractory DOC may be assumed to be 45  $\mu\text{M}$  with a  $\Delta^{14}\text{C}$  value of  $-477\text{‰}$ , and the  $\Delta^{14}\text{C}$  value of the surface produced fresh DOC similar with local  $\text{DI}^{14}\text{C}$  (about  $-150\text{‰}$ ) since the DIC is the ultimate carbon source for primary production. Using the average  $\Delta^{14}\text{C}$  value of  $-277\text{‰}$  at surface, input of fresh DOC via mass balance is estimated to be 71  $\mu\text{M}$  ( $45 \times (-477\text{‰}) + X \times (-150\text{‰}) = (45 + X) \times (-277\text{‰})$ ). However, average measured surface DOC concentration was much lower than the estimate (calculated bulk DOC concentration is 116  $\mu\text{M}$ ).

Here we try to address the mechanism responsible for the increased  $\Delta^{14}\text{C}$  values in the Amundsen polynya surface water with a small increase in DOC concentration. If I assume that the background was constant throughout the water column, a large discrepancy exists between the estimated  $\Delta^{14}\text{C}$  for surface DOC ( $-384\text{‰}$ ;  $63 \times (-431\text{‰}) = 18 \times (-150\text{‰}) + 45 \times (-477\text{‰})$ ) and our measurement (average of  $-277\text{‰}$ ). This discrepancy indicates that the assumption of constant background may not be correct. Thus consumption of a fraction of “refractory” old DOC delivered from deep water should be provoked. This assumption is consistent with Follett et

al (2014) that estimated radiocarbon composition of DOC at different depth.

Different from the previous vertical DOC composition schematic (Fig. 11A), I propose a new vertical DOC composition profile: the proportion of refractory, low  $\Delta^{14}\text{C}$  DOC decreases from the deep ocean to the surface (Fig. 11B). If the main contributors to surface DOC are refractory DOC ( $-477\text{‰}$ ) from deep water and primary production ( $-150\text{‰}$ ) input, each source should account for 38% and 62% of surface water DOC based on radiocarbon balance ( $-477\text{‰}\times 38\% - 150\text{‰}\times 62\% = -277\text{‰}$ ). This concentration of old DOC that used be considered as refractory in the deep water, decreases from the bottom ( $45\mu\text{M}$ ) to surface ( $24\mu\text{M}$ ): approximately 53% of deep DOC has been removed in the surface water.

The processes responsible for this removal of old DOC is unclear. One possibility is photochemical degradation, which has been suggested as the main sink of old DOC (Mopper et al., 1991). During the polynya open season, the surface water becomes exposed to strong sunlight, enriched in UV (Herman et al., 1996). An alternative explanation is that this deep DOC could be consumed by bacteria when it is mixed with high concentration of newly produced DOC. This is consistent with the mechanism proposed by Arrieta et al. (2015) that deep DOC concentration is too low to be utilized by bacteria instead of chemical recalcitrancy to microbial degradation.

Further research is needed to understand which process is responsible for the consumption of refractory DOC.

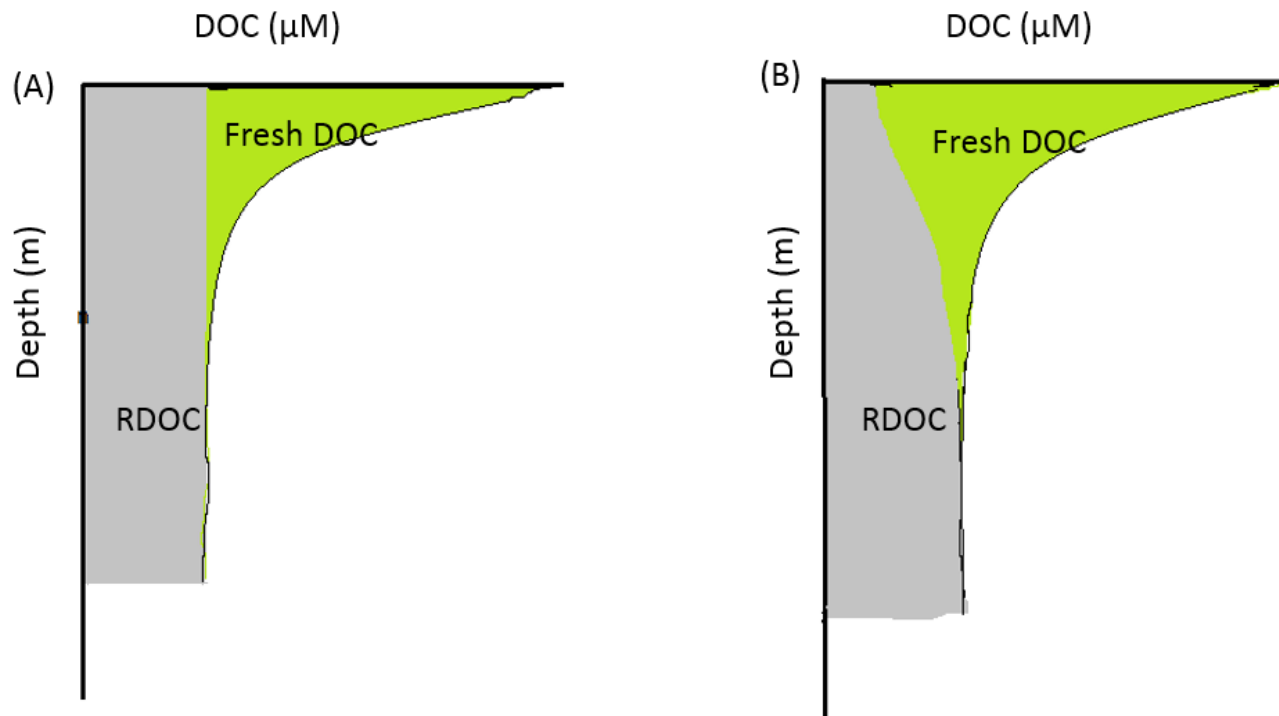


**Fig. 11.** Conceptual DOC cycling model. Gray shadow represents the refractory DOC (RDOC) and green shadow in the surface stands for the newly produced fresh DOC via photosynthesis. (A) The deep DOC is refractory and conserved throughout water column; (B) A fraction of refractory DOC is removed in the surface layer.

## 5. SUMMARY AND CONCLUSION

The  $\Delta^{14}\text{C}$  values of deep DOC collected from the Amundsen Sea were similar to the Southern Ocean mid depth water. However, the corresponding  $\delta^{13}\text{C}$  values with the mean value of  $-27.8\pm 0.8\%$  (n=11) at all depth were lower than that in other open ocean. These low  $\delta^{13}\text{C}$  values imply that a fraction of deep DOC was likely produced in the Amundsen Sea because organic matter produced in the Amundsen Sea was depleted in stable carbon isotope (Kim et al., 2015).

Based on the bulk  $\Delta^{14}\text{C}$  values of surface water DOC, the similarity in DOC concentration between the Amundsen polynya and sea ice zone suggested that DOC did not accumulate at the surface not because of low DOC production rate but because of high DOC consumption rate. The estimation of  $\Delta^{14}\text{C}$  values of additional source of DOC to the surface water based on two-endmember conserved mixing model revealed that primary production was the main contributor of additional source in the euphotic layer in the sea ice zone. Applying same analysis to the Amundsen polynya and Dotson Ice shelf site, the estimated  $\Delta^{14}\text{C}$  values of additional DOC source to the surface water were unreasonably high, suggesting that this approach was inappropriate in these region.

Spatial variability of  $\Delta^{14}\text{C}$  values at the surface could be partly explained by isopycnal mixing process, but the variation in  $\Delta^{14}\text{C}$  values at the same density suggest that other processes impact the spatial distribution of radiocarbon. The mass balance calculation based on radiocarbon in the Amundsen polynya surface water suggested that considerable amount of young DOC was added and a fraction of the old DOC was removed. Since DOC concentration was only slightly higher in the polynya than in the sea ice zone, a reasonable explanation is that a fraction of old DOC was consumed. The process responsible to the removal of old DOC from the surface water is not clear at the moment, although one can provoke UV irradiation and/or bacterial activity.

## 6. REFERENCES

- Aluwihare, L. I., Repeta, D. J., and Chen, R. F., 2002. Chemical composition and cycling of dissolved organic matter in the Mid-Atlantic Bight. *Deep Sea Research Part II: Topical Studies in Oceanography*, 49(20), 4421-4437.
- Arrieta, J. M., Mayol, E., Hansman, R. L., Herndl, G. J., Dittmar, T., and Duarte, C. M., 2015. Dilution limits dissolved organic carbon utilization in the deep ocean. *Science*, 348(6232), 331-333.
- Arrigo, K. R., and Van Dijken, G. L., 2003. Phytoplankton dynamics within 37 Antarctic coastal polynya systems. *Journal of Geophysical Research: Oceans*, 108(C8). doi:10.1029/2002JC001739
- Arrigo, K. R., van Dijken, G., and Long, M., 2008a. Coastal Southern Ocean: A strong anthropogenic CO<sub>2</sub> sink. *Geophysical Research Letters*, 35(21). doi:10.1029/2008GL035624
- Arrigo, K. R., van Dijken, G. L., and Bushinsky, S., 2008b. Primary production in the Southern Ocean, 1997–2006. *Journal of Geophysical Research: Oceans*, 113(C8). doi:10.1029/2007JC004551
- Arrigo, K. R., Lowry, K. E., and van Dijken, G. L., 2012. Annual changes in sea ice and phytoplankton in polynyas of the Amundsen Sea,

Antarctica. *Deep Sea Research Part II: Topical Studies in Oceanography*, 71, 5-15.

Bauer J E, Williams P M, Druffel E R M., 1992. 14C activity of dissolved organic carbon fractions in the north-central Pacific and Sargasso Sea. *Nature*, 357: 667-670.

Bauer, J. E., Druffel, E. R., Williams, P. M., Wolgast, D. M., and Griffin, S., 1998. Temporal variability in dissolved organic carbon and radiocarbon in the eastern North Pacific Ocean. *Journal of Geophysical Research: Oceans*, 103(C2), 2867-2881.

Bauer, J. E., Druffel, E. R., Wolgast, D. M., Griffin, S., and Masiello, C. A., 1998. Distributions of dissolved organic and inorganic carbon and radiocarbon in the eastern North Pacific continental margin. *Deep Sea Research Part II: Topical Studies in Oceanography*, 45(4), 689-713.

Beaupré, S. R., Druffel, E. R., and Griffin, S., 2007. A low-blank photochemical extraction system for concentration and isotopic analyses of marine dissolved organic carbon. *Limnology and Oceanography: Methods*, 5(JUN), 174 - 184.

Beaupré, S. R., and Aluwihare, L., 2010. Constraining the 2-component model of marine dissolved organic radiocarbon. *Deep Sea Research*

*Part II: Topical Studies in Oceanography*, 57(16), 1494-1503.

Boyd, P. W., 2002. ENVIRONMENTAL FACTORS CONTROLLING PHYTOPLANKTON PROCESSES IN THE SOUTHERN OCEAN1. *Journal of Phycology*, 38(5), 844-861.

Boyd, P. W., and Doney, S. C., 2002. Modelling regional responses by marine pelagic ecosystems to global climate change. *Geophysical Research Letters*, 29(16). doi:10.1029/2001GL014130

Calvin, M., Heidelberger, C., Reid, J. C., Tolbert, B. M., Yankwich, P. E., and Collins, C. J., 1949. Isotopic Carbon. *The Journal of Physical Chemistry*, 53(7), 1139-1140.

Carlson, C. A., Ducklow, H. W., and Hansel, D. A., 1998. Organic carbon partitioning during spring phytoplankton blooms in the Ross Sea polynya and the Sargasso Sea. *Oceanography*, 43(3), 375-386.

Carlson, C. A., 2002. Production and removal processes. *Biogeochemistry of marine dissolved organic matter*, 91-151.

Coale, K. H., Gordon, R. M., and Wang, X., 2005. The distribution and behavior of dissolved and particulate iron and zinc in the Ross Sea and Antarctic circumpolar current along 170 W. *Deep Sea Research Part I: Oceanographic Research Papers*, 52(2), 295-318.

Doval, M. D., Álvarez-Salgado, X. A., Castro, C. G., and Pérez, F. F., 2002.

- Dissolved organic carbon distributions in the Bransfield and Gerlache Straits, Antarctica. *Deep Sea Research Part II: Topical Studies in Oceanography*, 49(4), 663-674.
- Druffel, E. R., and Williams, P. M., 1990. Identification of a deep marine source of particulate organic carbon using bomb  $^{14}\text{C}$ . *Nature* 347, 172 – 174.
- Druffel, E. R., Williams, P. M., Bauer, J. E., and Ertel, J. R., 1992. Cycling of dissolved and particulate organic matter in the open ocean. *Journal of Geophysical Research: Oceans*, 97(C10), 15639-15659.
- Druffel, E. R., and Bauer, J. E., 2000. Radiocarbon distributions in Southern Ocean dissolved and particulate organic matter. *Geophysical research letters*, 27(10), 1495 - 1498. doi: 10.1029/1999GL002398.
- Druffel, E. R. M., and Griffin, S., 2015. Radiocarbon in dissolved organic carbon of the South Pacific Ocean. *Geophysical Research Letters*, 42(10), 4096-4101.
- Ducklow, H. W., Steinberg, D. K., and Buesseler, K. O., 2001. Upper ocean carbon export and the biological pump. *OCEANOGRAPHY-WASHINGTON DC-OCEANOGRAPHY SOCIETY*, 14(4), 50-58.
- Ducklow, H. W., Wilson, S. E., Post, A. F., Stammerjohn, S. E., Erickson,

- M., Lee, S., Lowry, K. E., Sherrell, R. E., Yager, P. L., 2015. Particle flux on the continental shelf in the Amundsen Sea Polynya and Western Antarctic Peninsula. *Elementa: Science of the Anthropocene*, 3(1), 000046. doi: 10.12952/journal.elementa.000046
- Follett, C. L., Repeta, D. J., Rothman, D. H., Xu, L., and Santinelli, C., 2014. Hidden cycle of dissolved organic carbon in the deep ocean. *Proceedings of the National Academy of Sciences*, 111(47), 16706-16711.
- Gerringa, L. J., Alderkamp, A. C., Laan, P., Thuroczy, C. E., De Baar, H. J., Mills, M. M., van Dijken, G., van Haren, H., Arrigo, K. R., 2012. Iron from melting glaciers fuels the phytoplankton blooms in Amundsen Sea (Southern Ocean): Iron biogeochemistry. *Deep Sea Research Part II: Topical Studies in Oceanography*, 71, 16-31.
- Godwin, H., 1962. Half-life of radiocarbon. *Nature*, 195,984.
- Giannelli, V., Thomas, D. N., Haas, C., Kattner, G., Kennedy, H., Dieckmann, G. S., 2001. Behaviour of dissolved organic matter and inorganic nutrients during experimental sea-ice formation. *Annals of Glaciology*, 33(1), 317-321.
- Hansell, D. A., and Carlson, C. A., 1998. Deep-ocean gradients in the

concentration of dissolved organic carbon. *Nature*, 395(6699), 263-266.

Hansell, D. A., Carlson, C. A., Repeta, D. J., Schlitzer, R., 2009. Dissolved organic matter in the ocean: A controversy stimulates new insights. **Oceanography** 22(4):202–211.

Hansell, D. A., 2013. Recalcitrant dissolved organic carbon fractions. *Marine Science*, 5:421-425.

Hansell, D. A., and Carlson, C. A., 2013. Localized refractory dissolved organic carbon sinks in the deep ocean. *Global Biogeochemical Cycles*, 27(3), 705-710.

Hedges, J. I., 1992. Global biogeochemical cycles: progress and problems. *Marine chemistry*, 39(1), 67-93.

Hedges, J. I., Keil, R. G., and Benner, R., 1997. What happens to terrestrial organic matter in the ocean?. *Organic geochemistry*, 27(5), 195-212.

Herman, J. R., Bhartia, P. K., Ziemke, J., Ahmad, Z., and Larko, D., 1996. UV - B increases (1979–1992) from decreases in total ozone. *Geophysical Research Letters*, 23(16), 2117-2120.

Hwang, J., Druffel, E. R., and Bauer, J. E., 2006. Incorporation of aged dissolved organic carbon (DOC) by oceanic particulate organic

- carbon (POC): an experimental approach using natural carbon isotopes. *Marine Chemistry*, 98(2), 315-322.
- Jacobs, S. S., Jenkins, A., Giulivi, C. F., and Dutrieux, P., 2011. Stronger ocean circulation and increased melting under Pine Island Glacier ice shelf. *Nature Geoscience*, 4(8), 519-523.
- Jenkins, A., Dutrieux, P., Jacobs, S. S., McPhail, S. D., Perrett, J. R., Webb, A. T., and White, D., 2010. Observations beneath Pine Island Glacier in West Antarctica and implications for its retreat. *Nature Geoscience*, 3(7), 468-472.
- Jumars, P. A., Penry, D. L., Baross, J. A., Perry, M. J., and Frost, B. W., 1989. Closing the microbial loop: dissolved carbon pathway to heterotrophic bacteria from incomplete ingestion, digestion and absorption in animals. *Deep Sea Research Part A. Oceanographic Research Papers*, 36(4), 483-495.
- Kim, M., Hwang, J., Kim, H. J., Kim, D., Yang, E. J., Ducklow, H. W., Hyung, S. L., Lee, S. H., Prak, J., and Lee, S., 2015. Sinking particle flux in the sea ice zone of the Amundsen shelf, Antarctica. *Deep Sea Research Part I: Oceanographic Research Papers*, 101, 110-117.
- Kim, M., Hwang, J., Lee, S. H., Kim, H. J., Kim, D., Yang, E. J., & Lee, S.,

2016. Sedimentation of particulate organic carbon on the Amundsen Shelf, Antarctica. *Deep Sea Research Part II: Topical Studies in Oceanography*, 123, 135-144.
- Libbey, W. F., 1952. Radiocarbon dating. *University of Chicago Press*, 218-222.
- Lide, D. R., 2007. Handbook of Chemistry and Physics, volume 88th edition. *CRC Press*, 22(24), 154.
- McCarthy, M. D., Hedges, J. I., and Benner, R., 1998. Major bacterial contribution to marine dissolved organic nitrogen. *Science*, 281(5374), 231-234.
- McNichol, A. P., Osborne, E. A., Gagnon, A. R., Fry, B., and Jones, G. A., 1994. TIC, TOC, DIC, DOC, PIC, POC—Unique aspects in the preparation of oceanographic samples for <sup>14</sup>C-AMS. *Nuclear Instruments and Methods in Physics Research Section B: Beam Interactions with Materials and Atoms*, 92(1-4), 162-165.
- McNichol, A. P., and Aluwihare, L. I., 2007. The power of radiocarbon in biogeochemical studies of the marine carbon cycle: Insights from studies of dissolved and particulate organic carbon (DOC and POC). *Chemical reviews*, 107(2), 443-466.
- Mopper, K., Zhou, X., Kieber, R. J., Kieber, D. J., Sikorski, R. J., and Jones,

- R. D., 1991. Photochemical degradation of dissolved organic carbon and its impact on the oceanic carbon cycle. *Nature*, 353, 60-62.
- Mortazavi, B., and Chanton, J. P., 2004. Use of Keeling plots to determine sources of dissolved organic carbon in nearshore and open ocean systems. *Limnology and oceanography*, 49(1), 102-108.
- Ogawa, H., Amagai, Y., Koike, I., Kaiser, K., and Benner, R., 2001. Production of refractory dissolved organic matter by bacteria. *Science*, 292(5518), 917-920.
- Opsahl, S., and Benner, R., 1997. Distribution and cycling of terrigenous dissolved organic matter in the ocean. 480-482.
- Parkinson, C. L., and Cavalieri, D. J., 2012. Antarctic sea ice variability and trends, 1979–2010. *The Cryosphere*, 6(4), 871-880.
- Poulton, S. W., and Raiswell, R., 2005. Chemical and physical characteristics of iron oxides in riverine and glacial meltwater sediments. *Chemical Geology*, 218(3), 203-221.
- Repeta, D. J., and Aluwihare, L. I., 2006. Radiocarbon analysis of neutral sugars in high-molecular-weight dissolved organic carbon: Implications for organic carbon cycling. *Limnology and oceanography*, 51(2), 1045-1053.

- Rignot, E., and Jacobs, S. S., 2002. Rapid bottom melting widespread near Antarctic ice sheet grounding lines. *Science*, 296(5575), 2020-2023.
- Rignot, E., Bamber, J. L., Van Den Broeke, M. R., Davis, C., Li, Y., Van De Berg, W. J., and Van Meijgaard, E., 2008. Recent Antarctic ice mass loss from radar interferometry and regional climate modelling. *Nature Geoscience*, 1(2), 106-110.
- Rignot, E., Mouginot, J., Morlighem, M., Seroussi, H., and Scheuchl, B., 2014. Widespread, rapid grounding line retreat of Pine Island, Thwaites, Smith, and Kohler glaciers, West Antarctica, from 1992 to 2011. *Geophysical Research Letters*, 41(10), 3502-3509..
- Roy, T., Rayner, P., Matear, R., and Francey, R., 2003. Southern hemisphere ocean CO<sub>2</sub> uptake: reconciling atmospheric and oceanic estimates. *Tellus B*, 55(2), 701-710.
- Sabine, C. L., Feely, R. A., Gruber, N., Key, R. M., Lee, K., Bullister, J. L., Wanninkhof, R., Wong, C. S., Wallace, D.W.R., Tilbrook, B., Millero, F.J., Peng, T., Kozyr, A., Ono, T., and Rios, A. F., 2004. The oceanic sink for anthropogenic CO<sub>2</sub>. *science*, 305(5682), 367-371.
- Sipler, R. E., and Connelly, T. L., 2015. Bioavailability of surface dissolved organic matter to aphotic bacterial communities in the Amundsen

Sea Polynya, Antarctica. *Elementa: Science of the Anthropocene*, 3(1), 000060.  
doi:10.12952/journal.elementa.000060

Stammerjohn, S., Massom, R., Rind, D., and Martinson, D., 2012. Regions of rapid sea ice change: An inter-hemispheric seasonal comparison. *Geophysical Research Letters*, 39(6). doi:10.1029/2012GL050874

Stuiver, M. and Polach, H. A., 1977. Discussion; reporting of C-14 data. *Radiocarbon*, 19(3), 355-363.

Suess, H. E., 1955. Radiocarbon concentration in modern wood. *Science*, 122 (3166), 415-417.

Takahashi, T., Sutherland, S. C., Sweeney, C., Poisson, A., Metzler, N., Tilbrook, B., Bates, N., Wanninkhof, R., Feely, R. A., Sabine, C., Olafsson, J. and Nojiri, Y., 2002. Global sea-air CO<sub>2</sub> flux based on climatological surface ocean pCO<sub>2</sub>, and seasonal biological and temperature effects. *Deep Sea Research Part II: Topical Studies in Oceanography*, 49(9), 1601-1622.

Thomas, D. N., Lara, R. J., Eicken, H., Kattner, G. and Skoog, A., 1995. Dissolved organic matter in Arctic multi-year sea ice during winter: major components and relationship to ice characteristics. *Polar*

*Biology*, 15(7), 477-483.

Thomas, D. N., Lara, R. J., Eicken, H., Kattner, G. and Skoog, A., 1995.

Dissolved organic matter in Arctic multi-year sea ice during winter: major components and relationship to ice characteristics. *Polar Biology*, 15(7), 477-483.

Wåhlin, A. K., Yuan, X., Björk, G., and Nohr, C., 2010. Inflow of Warm Circumpolar Deep Water in the Central Amundsen Shelf. *Journal of Physical Oceanography*, 40(6), 1427-1434.

Wåhlin, A. K., Kalén, O., Arneborg, L., Björk, G., Carvajal, G. K., Ha, H. K., Kim, T. W., Lee, S.H., Lee, J. H. and Stranne, C., 2013. Variability of warm deep water inflow in a submarine trough on the Amundsen Sea shelf. *Journal of Physical Oceanography*, 43(10), 2054-2070.

Walker, D. P., Brandon, M. A., Jenkins, A., Allen, J. T., Dowdeswell, J. A. and Evans, J., 2007. Oceanic heat transport onto the Amundsen Sea shelf through a submarine glacial trough. *Geophysical Research Letters*, 34(2). doi:10.1029/2006GL028154

Wedborg, M., Hoppema, M., and Skoog, A., 1998. On the relation between organic and inorganic carbon in the Weddell Sea. *Journal of Marine Systems*, 17(1), 59-76.

- Wiebinga, C. J., and De Baar, H. J. W., 1998. Determination of the distribution of dissolved organic carbon in the Indian sector of the Southern Ocean. *Marine Chemistry*, 61(3), 185-201.
- Williams, P. M., and Druffel, E. R., 1987. Radiocarbon in dissolved organic matter in the central North Pacific Ocean. *Nature*, 330(6145), 246-248.
- Yager, P.L., Sherrell, L.M., Stammerjohn, S.E., Alderkamp, A.C., Schofield, O., Abrahamsen, E.P., Arrigo, K.R., Bertilsson, S., Garay, D., Guerrero, R., Lowry, K.E., Mosknes, P.O., Ndungu, K., Post, A.F., Randall-Goodwin, E., Riemann, L., Severmann, S., Thatje, S., van Dijken, G.L. and Wilson, S., 2012. ASPIRE: The Amundsen Sea Polynya International Research Expedition. *Oceanography*, 25, (3), 40-53.

## ABSTRACT (IN KOREAN)

해양 용존유기탄소는 가장 환원된 탄소 저장고 중 하나로 전지구적인 탄소 순환에 중요한 역할을 한다. 탄소 동위원소 비는 남극 아문젠해 용존유기탄소의 기원과 운명을 조사하기 위해 추적자로 사용되었다.  $\Delta^{14}\text{C}$  값은  $-260$  와  $-481$  ‰ 사이였다.  $\Delta^{14}\text{C}$  값은 심층보다 상층 높았고  $\Delta^{14}\text{C}$  최대값은 20 m 깊이의 아문젠해 폴리냐에서 발견되었다.  $^{14}\text{C}$  나이의 큰 공간적인 변화가 세 개의 정점에 걸쳐 혼합층 내에서 관찰되었다. 용존유기탄소의 농도는 아문젠해 해빙역보다 폴리냐 표층에서 매우 높았으며 오래된 용존유기탄소의 분별이 상층에서 제거되었음을 암시하였다. 아문젠해 내 채취한 모든 시료는 대양에 비해  $^{13}\text{C}$  비가 낮았다.  $\delta^{13}\text{C}$  값의 평균값은  $-27.8 \pm 0.8$  ‰ (n=11)로  $-26.2$  와  $-28.9$  ‰ 사이였다.  $\delta^{13}\text{C}$  과  $\Delta^{14}\text{C}$  분포는 아문젠해 폴리냐가 오래된 용존유기탄소를 제거할 수 있음을 제시한다.

**주요어** : 용존유기탄소, 방사성탄소, 탄소 안정동위원소, 폴리냐, 아문젠해

**학 번** : 2014-25134